ENVELOP ENRICHMENT METHOD TO APPLY PERIODIC BOUNDARY CONDITIONS ON NON-PERIODIC UNIT CELLS

Florian Vazeille[1], Louis Laberge Lebel[1,*]

[1] Advanced Composites and Fibers Structures Laboratory (ACFSlab), High Performance Polymer and Composite Systems (CREPEC), Polytechnique Montreal, 2900 Blvd. Édouard-Montpetit, Montréal, Québec H3T 1J4, Canada
*corresponding author: LLL@polymtl.ca

Keywords: Periodic Boundary Condition, Representative Volume Element, Envelope Enrichment Method, Braided composite Reinforcement, Finite elements

ABSTRACT

In the field of composite material engineering, accurately predicting mechanical behaviour is essential for tailoring performance in various applications. This paper presents a novel approach to homogenize composite materials for accurate prediction of their mechanical performance. The proposed method focuses on non-periodic representative volume elements (RVEs), which present challenges in applying classic periodic boundary conditions. This is due to the varying properties of the elements at the boundary and irregular meshing. To address this issue, we introduce an envelope surrounding the RVE, onto which periodic conditions are applied. An iterative process is required to compute the stiffness tensor of the envelope until a convergence is observed. The stiffness tensor is computed using the perturbation homogenization technique implemented into the Finite Element Analysis (FEA).. The method is validated on non-periodic arrangements of spherical inclusions embedded within a matrix. The prediction of the elastic properties of Ultra-High Molecular Weight Polyethylene (UHMWPE) mixed into a polypropylene matrix is conducted for a volume fraction up to 35%.

1 INTRODUCTION

Composite materials blending discrete reinforcements into a continuous polymer matrix, have gained significant attention due to their potential to achieve tailored mechanical performance for various applications [1,2]. These materials can be isotropic or anisotropic, depending on the reinforcement used, such as fibres or particles, and their arrangement. Moreover, other factors such as the shape of the reinforcement, proportion of the constituents, quality of the interface, production process are other examples of many more that can influence the composite material's properties. In this context, understanding the microstructural behaviour of composite materials is crucial, as it plays a dominant role in determining their overall performance.

A common approach to investigating the mechanical properties of composites is through numerical simulations of a Representative Volume Element (RVE) [3,4], that is, a microscopic sample that exhibits the same mechanical properties as the entire composite structure. Discretization at the microscale level is therefore often necessary for complex structures, and multi-scale analysis is employed for determining a variety of properties. Tensile strength is one of the primary features analysed through homogenization. Mean field homogenization [5–7] relies on basic mathematical relationships and geometrical assumptions, while full field homogenization [8–11] depends on a clear definition of the microstructure and characteristics of the interactions at the boundary of phases.

Integrating homogenization into the Finite Element (FE) framework allows for multi-scale analysis and characterization of macroscopic behaviour. The convergence on the homogenized properties was demonstrated to be faster using periodic boundary conditions along with RVE size [12]. However, applying the RVE method to non-periodic structures poses challenges, as it becomes difficult to apply classic boundary conditions on nodes belonging on elements with varying properties and when the mesh is not periodic [13–15]. A few existing studies [12,16] employ a technique, herein referred to as Envelope Enrichment (EE). A dummy material is created around the original RVE to create a support domain suitable for the application of PBCs. Through an iterative process, the homogenized properties of the enveloped RVE are assigned to the envelope until convergence of those properties is observed.

This paper aims to compare the results of the EE method and those obtained from other empirical micromechanics models Voigt, Reuss, and Halpin–Tsai, and Asymptotic Homogenization (AH) from another study [17]. The EE method will first be described, and its implementation will be specified. A work case will be presented with spherical particles of Ultra High Molecular Weight Polyethylene (UHMWPE) dispersed into Polypropylene (PP). The results are then compared.

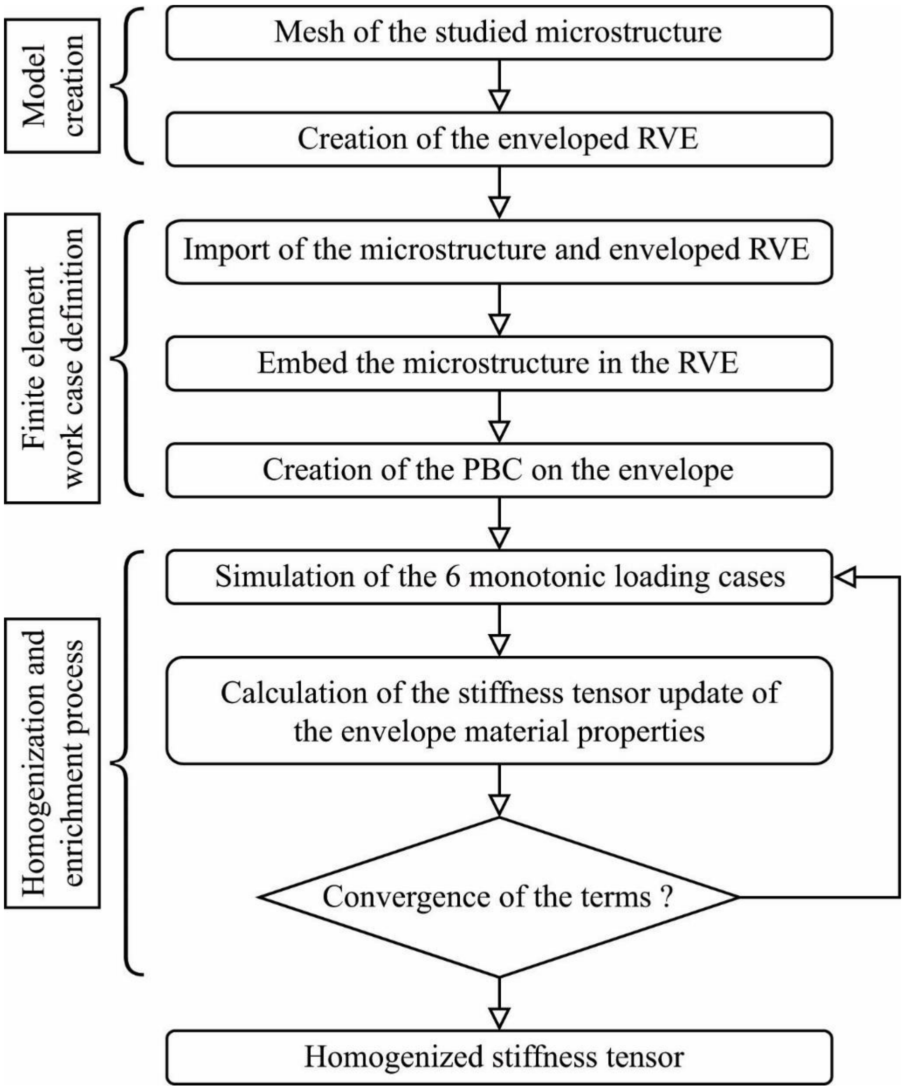

Figure 1: Illustration of the method implementation for the homogenization

2 DESCRIPTION OF THE METHOD

Figure 1 shows the complete process to compute the homogenized properties of a non-periodic composite model using the EE method. The following sections present each step of the method.

2.1 Model creation

Figure 2 illustrates the model creation starting from the geometry of the inclusions. A classic RVE is added to create the host region where the inclusions reside. The RVE is meshed, and the properties of the host matrix are assigned. The inclusions are meshed with inclusions' properties. The inclusion mesh is overlaid to the RVE mesh. The embedding technique is employed to link the inclusion to the RVE host matrix, assuming a perfect mechanical interaction between the inclusions and the hots matrix. More information on the embedding technique can be found in [18,19]. The envelope is added around the RVE with a periodicity constraint on the outside boundary. A material with arbitrary properties is applied to the envelope. The final model is meshed to be studied through computational simulation using FEA. This ensure the presence of a periodic mesh onto which PBC can be applied.

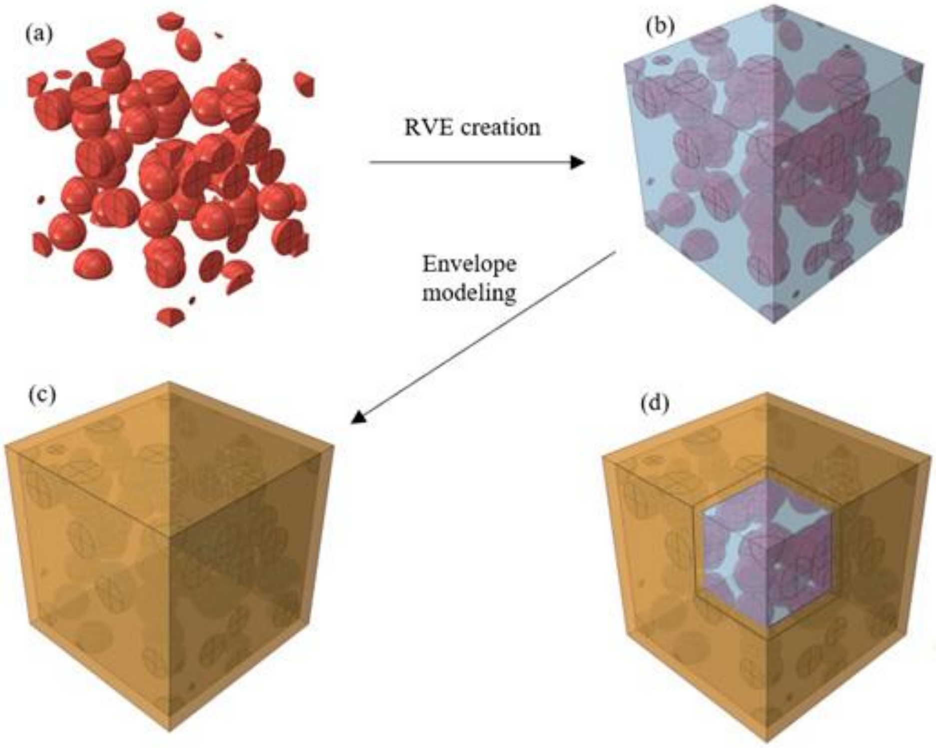

Figure 2: Illustration of the model creation: (a) Input model of the inclusions geometry , (b)Creation of a RVE, (c) Creation of the envelop of material with arbitrary properties. (d) Illustration of a the final enveloped model with a corner of the envelop being cut.

2.2 Homogenization

The strategy implemented consists of formulating the localization problems associated with PBCs by introducing additional reference points supporting the components of the macroscopic deformations. The specific boundary conditions are imposed via linear relations between the degrees of freedom of the contour nodes and these additional DOFs applied on three arbitrary reference points. It can then be shown that the nodal forces associated with the DOFs supporting the components of the mean strains are equal to the components of the mean stress in the total volume.

Given the presence of heterogeneities in a finitely deformable heterogeneous macro-structure $\mathcal{M}$, the solution of the Boundary Value Problem (BVP) is highly oscillatory. Solving such problems appears very challenging in its original form detailed in [20] and requires replacing $\mathcal{M}$ with a corresponding homogeneous replica $\mathcal{M}*$.When dealing with RVEs, the work criterion originally expressed by [21] leads to the definition of the macroscopic volume average of the controlled deformation gradient F and the 1st Piola–Kirchhoff stress tensor P They are expressed as the volume average of their microscopic counterpart over the total volume V_0 of the RVE:

$$F = \langle f \rangle = \frac{1}{|V_0|} * \int_{V_0} f \, dV, \quad P = \langle p \rangle = \frac{1}{|V_0|} * \int_{V_0} p \, dV \tag{1}$$

For better clarity the macroscopic (resp. microscopic) quantities are expressed with UPPERCASE (resp. lowercase) letter and symbols. The work criterion is satisfied when periodic boundary conditions are applied such as:

$$x - x_0 = F(X - X_0) \tag{2}$$

where x and X denote the position vectors for the current and reference configurations. To do so in the FEM framework, reference points are used to support the displacement representing the Cartesian components of the macroscopic displacement gradient U such that on the microscopic scale:

$$u_j^{n_i^+} - u_j^{n_i^-} = \lambda_j \nabla U_{ji} \qquad i,j \in \{1,2,3\} \tag{3}$$

with λ_j the dimensions of the cuboid

Those conditions are introduced onto three reference points supporting the macroscopic displacement gradient. This is done by imposing a displacement on those reference points $R_{p\in\{1,2,3\}}$ which gives:

$$v_p = \nabla U_{jp} \tag{4}$$

The anti-symmetry of the boundary tractions is automatically satisfied such that the nodal forces on oppositely located nodes are of equal magnitude and opposite sign when these homogeneous constraints are enforced through Lagrange multipliers, which correspond, aside from sign to the nodal forces of the boundary nodes. The weak form of the boundary value problem on the equivalent homogeneous microstructure $\mathcal{M}^*$ can be expressed in the form:

$$\int_{V_0} P \cdot \delta F dV = \sum_{k,p=1}^{3} R_p \delta v_k \tag{5}$$

which gives that the reaction forces R_p measured on the reference points correspond to the macroscopic Piola-Kirchhoff stresses over the volume V_0.

2.3 Implementation of EE in FEA

To overcome the challenge of non-periodic mesh for complex materials, an RVE encapsulated into an envelope is created and meshed to be studied with FEA. All the meshing work is done with the python solver from GMSH [22], an open-source three-dimensional finite element grid generator. The actual method developed can deal with any existing microstructure mesh file in the input format used by Abaqus. The envelope is generated around the RVE with a periodicity of the mesh applied on the outside boundary of the envelope thanks to an affine transformation matrix. This, coupled to a transfinite constraint explicitly specifying the location of the nodes on each edge ensures the presence of a pair of nodes facing each other on every parallel face of the envelope. This method allows the continuity of the mesh between the RVE and the envelope in such a way that each node on the contact surfaces is shared between both entities. The change of mesh density is therefore not problematic as there is no discontinuity generated, while still maintaining the necessary periodic constraints.

To conduct the homogenization process, the Homtools [23] plugin implemented into Abaqus/CAE is employed. Only linear problems are considered, which is true for RVE simulation within the elastic domain of its components. Hence, the principle behind the Abaqus framework is based on the Jaumann rate of the Kirchhoff stress tensor. Thanks to Homtools, equation (4) is applied automatically by creating a set of Multi-point Constraint (MPC) in Abaqus, linking each node pair $(n_{i-} n_{i+})$ on a periodic mesh.

Abaqus is used to define the model and run the different simulations. The original source code from Homtools is modified to be integrated into the actual workflow for a streamlined process. For each step of the enrichment process, 6 monotonic loading cases are calculated into different jobs. As the second Piola-Kirchhoff stress tensor is linked to the deformation tensor:

$$\Delta P = C_{ijkl} : \Delta F \tag{6}$$

Following equation (5) and assuming an anisotropic behaviour of the microstructure, the reaction forces are evaluated on the 3 reference points and the stiffness tensor C_{ijkl} is calculated at each step.

Using the Voigt notation, the problem can be written as follows:

$$\begin{bmatrix} C_{11} & C_{12} & C_{13} & C_{14} & C_{15} & C_{16} \\ C_{21} & C_{22} & C_{23} & C_{24} & C_{25} & C_{26} \\ C_{31} & C_{32} & C_{33} & C_{34} & C_{35} & C_{36} \\ C_{41} & C_{42} & C_{43} & C_{44} & C_{45} & C_{46} \\ C_{51} & C_{52} & C_{53} & C_{54} & C_{55} & C_{56} \\ C_{61} & C_{62} & C_{63} & C_{64} & C_{65} & C_{66} \end{bmatrix} * \begin{bmatrix} 1 \\ 0 \\ 0 \\ 0 \\ 0 \\ 0 \end{bmatrix} = \begin{bmatrix} \Delta P_1 \\ \Delta P_2 \\ \Delta P_3 \\ \Delta P_4 \\ \Delta P_5 \\ \Delta P_6 \end{bmatrix} \tag{6}$$

This depicts the calculation of the first column. The other columns can be calculated in an analogous manner and in parallel for more efficiency. The computed stiffness tensor is used to update the envelop properties. This process is repeated until a convergence of the terms is observed.

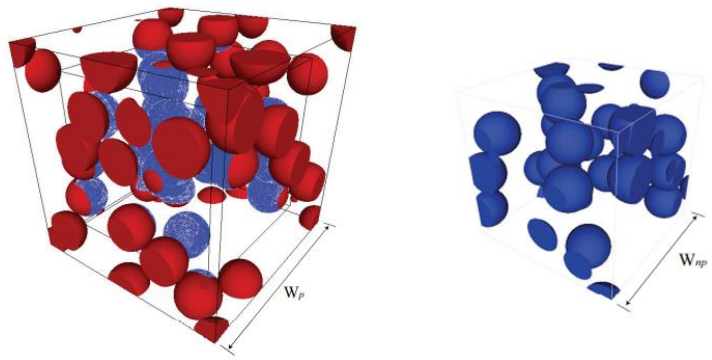

Figure 3: Illustration of the creation of the non-periodic RVE from a periodic RVE of randomly generated spheres

3 WORK-CASE

Figure 3 shows the periodic and the non-periodic models. The spherical inclusions have been generated with Mote3D [24], a toolbox creating randomly positioned spherical particles. Those inclusions are within a periodical cubical computational domain. This is done through an iterative process which inherently limits the total Volume Fraction (VF) which is comprised in the range [0.18;0.35] for the current study. The particle radius is set as a constant and equal to r = 10µm. No interpenetration is permitted between each particle inside the RVE with a width WP = 50µm. The number of inclusions is modified to adjust the VF parameter. To evaluate the developed method on non-periodic medium, the cubical domain was cropped to a smaller width $W_{np} = 38\mu m < W_p - r/2$. This way the periodicity property was annihilated. The effective properties of the periodic models were calculated directly with the Homtools plugin whereas the EE method was used for the non-periodic counterpart.

Properties	Polypropylene	UHMWPE
Elastic Modulus (GPA)	1.325	25.0
Shear Modulus (GPA)	0.432	10.4
Poisson's Ratio	0.43	0.20

Table 1: Properties of Polypropylene (PP) and ultra-high molecular weight polyethylene (UHMWP)

Figure 4 illustrate the meshed model of an enveloped RVE with embedded spherical inclusions. The slight offset between the matrix and the envelope material allows the creation of PBC constraints on a mesh with an imposed periodicity and matching nodes on opposite sides with uniform properties. The material properties of each section, matrix, inclusions, and envelope are assigned accordingly with the values detailed in Table 1.

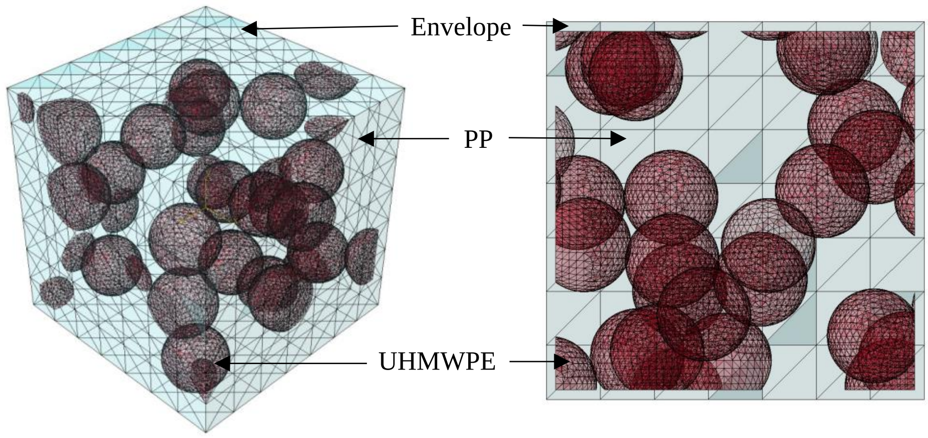

Figure 4: Illustration of a meshed enveloped RVE, with embedded spherical inclusions

4 RESULTS AND DISCUSSION

Figures 4 shows the evolution of the elastic modulus. The Voigt and Reuss models are known to give an upper and lower bound of the elastic modulus. Halpin Tsai considers the shape and arrangement of the particles which gives a better result in this case. Empirical and semi empirical micromechanics models rely heavily on the constituent's volume fraction. Therefore, Voigt, Reuss and Halpin Tsai all demonstrate a linear evolution according to VF for the elastic and shear modulus. Because UHMWPE has a higher tensile modulus than PP, the homogenized modulus increases with increasing VF. The AH results are extracted from another study [11], conducted on conformal mesh with the Finite Element Method (FEM) and follow closely the results obtained with the Halpin Tsai model. Periodic and non-periodic microstructures, homogenized with Homtools and the perturbation technique, shows higher values while being below the Voigt model.

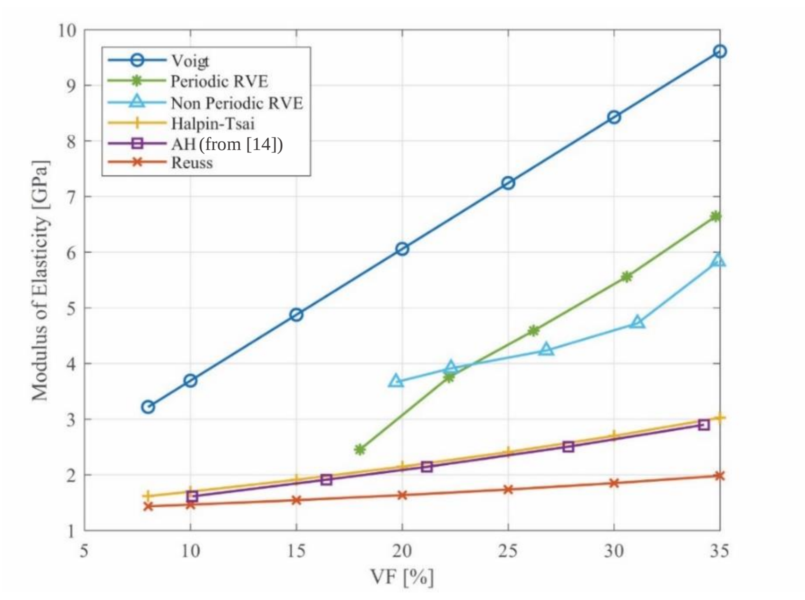

Figure 5: Elastic modulus according to the volume fraction predicted by various models: Voigt, Reuss, Halpin–Tsai, AH, periodic and non-periodic FE method.

Figure 6 depicts the shear modulus and Poisson's ration for the different models. Similar results are observed for the shear modulus and the modulus of elasticity. In the case of the Poisson ratio, the periodic and non-periodic results are closer to the expected value of the semi empirical models. The values for a VF over 25% are in good accordance with the other empirical models which was not the case for the AH. However, below 25% of VF, the EE method lies outside the Voigt and Reuss bounds. The underlying causative factors for the observed result remain ambiguous, despite the accurate measurements obtained for both the elastic and shear moduli. A comprehensive investigation into the off-diagonal components of the stiffness tensor may provide insights for elucidating this phenomenon.

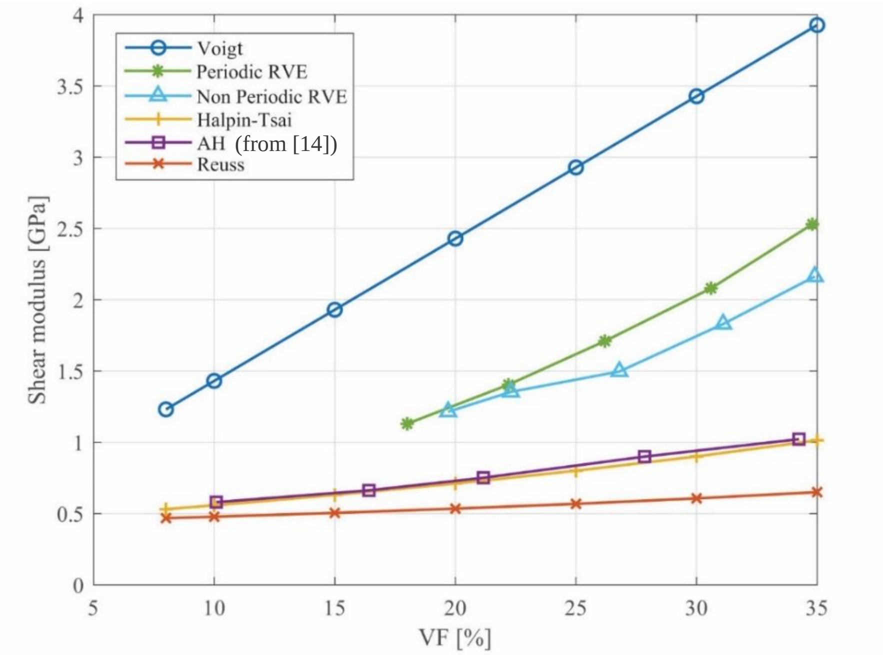

(a)

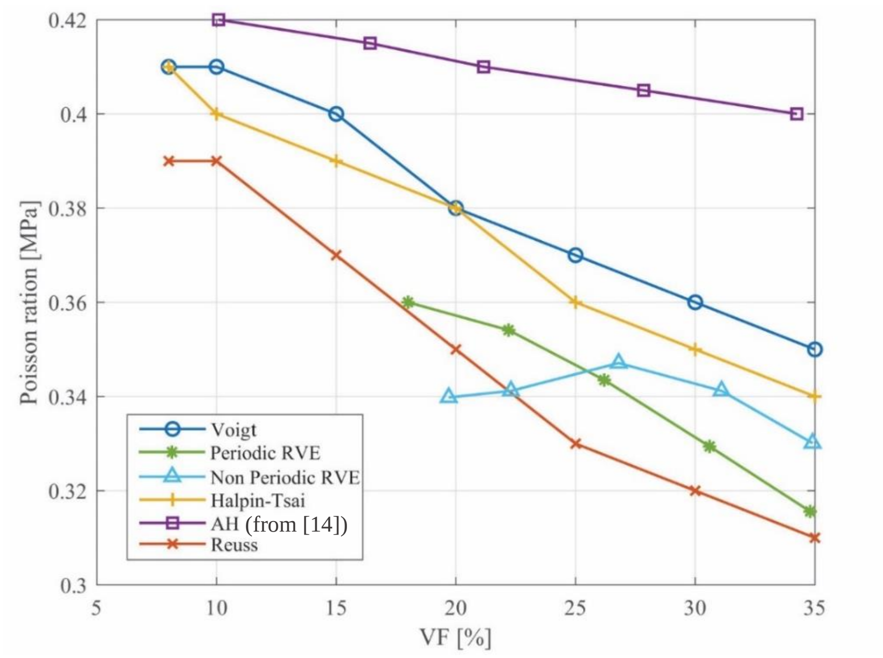

(b)

Figure 6: Shear modulus (a) and Poisson ratio (b) according to the volume fraction predicted by various models: Voigt, Reuss, Halpin–Tsai, AH, periodic and non-periodic FE method.

5 CONCLUSIONS

The present study demonstrated the EE method for predicting the effective properties of a composite material with spherical inclusions inside a polymer matrix. Spherical inclusions of UHMWPE are embedded in a polypropylene matrix and the resulting material was assumed to have an isotropic behaviour at the macroscale. The EE method demonstrates a convergence of the elastic properties and are close to the classical method. Those results where compared to analytical models, Voigt, Reuss and Halpin Tsai along with the results of another study employing the RVE within the finite element framework and AH. The results observed with the EE method show a good consistency with the original model while having a smaller mesh domain to work with. The EE results are found within the Voigt and Reuss bound for the shear and elastic modulus while being a little higher than the one from the Halpin Tsai model. Future work focusing on real life testing is needed to determine the accuracy of the results and whether the method can define a high bound more relevant than the one provided by the Voigt model. A review study of the envelope parameters such as thickness and mesh density should also determine the right setup to obtain the stiffness tensor of a given microstructure.

ACKNOLEGMENT

This work was supported by The Natural Sciences and Engineering Research Council of Canada [NSERC, RDCPJ 543847-19]; PRIMA Quebec [R18-13-003]; FilSpec Inc; Pultrusion Techniques; and Bauer Hockey ltd.

REFERENCES

[1] Rajak DK, Pagar DD, Kumar R, Pruncu CI. Recent progress of reinforcement materials: a comprehensive overview of composite materials. J Mater Res Technol 2019;8:6354–74. https://doi.org/10.1016/j.jmrt.2019.09.068.

[2] van de Werken N, Tekinalp H, Khanbolouki P, Ozcan S, Williams A, Tehrani M. Additively manufactured carbon fiber-reinforced composites: State of the art and perspective. Addit Manuf 2020;31:100962. https://doi.org/10.1016/j.addma.2019.100962.

[3] Walters DJ, Luscher DJ, Yeager JD. Considering computational speed vs. accuracy: Choosing appropriate mesoscale RVE boundary conditions. Comput Methods Appl Mech Eng 2021;374:113572. https://doi.org/10.1016/j.cma.2020.113572.

[4] He TL, Karamian P, Choï D. A Fictitious Domain Method for Numerical Homogenization n.d.

[5] Mori T, Tanaka K. Average stress in matrix and average elastic energy of materials with misfitting inclusions. Acta Metall 1973;21:571–4. https://doi.org/10.1016/0001-6160(73)90064-3.

[6] Benveniste Y. A new approach to the application of Mori-Tanaka's theory in composite materials. Mech Mater 1987;6:147–57. https://doi.org/10.1016/0167-6636(87)90005-6.

[7] Affdl JCH, Kardos JL. The Halpin-Tsai equations: A review. Polym Eng Sci 1976;16:344–52. https://doi.org/10.1002/pen.760160512.

[8] Gélébart L, Mondon-Cancel R. Non-linear extension of FFT-based methods accelerated by conjugate gradients to evaluate the mechanical behavior of composite materials. Comput Mater Sci 2013;77:430–9. https://doi.org/10.1016/j.commatsci.2013.04.046.

[9] Gélébart L, Derouillat J, Chen Y, Chateau C, Bornert M, King A, et al. Simulations FFT massivement parallèles en mécanique des matériaux hétérogènes, 2017.

[10] Moulinec H, Suquet P. A FFT-Based Numerical Method for Computing the Mechanical Properties of Composites from Images of their Microstructures. In: Pyrz R, editor. IUTAM Symp. Microstruct.-Prop. Interact. Compos. Mater., Dordrecht: Springer Netherlands; 1995, p. 235–46. https://doi.org/10.1007/978-94-011-0059-5_20.

[11] de Macedo RQ, Ferreira RTL, Donadon MV, Guedes JM. Elastic properties of unidirectional fiber-reinforced composites using asymptotic homogenization techniques. J Braz Soc Mech Sci Eng 2018;40:255. https://doi.org/10.1007/s40430-018-1174-9.

[12] Ye Z, Yu W. Maximize Unit Cell Choices for Variational Asymptotic Homogenization. 2012. https://doi.org/10.2514/6.2012-2002.

[13] Griffiths E, Bargmann S, Reddy BD. Elastic behaviour at the nanoscale of innovative composites of nanoporous gold and polymer. Extreme Mech Lett 2017;17. https://doi.org/10.1016/j.eml.2017.09.006.
[14] Wang R, Zhang L, Hu D, Liu C, Shen X, Cho C, et al. A novel approach to impose periodic boundary condition on braided composite RVE model based on RPIM. Compos Struct 2017;163:77–88. https://doi.org/10.1016/j.compstruct.2016.12.032.
[15] Larsson F, Runesson K, Saroukhani S, Vafadari R. Computational homogenization based on a weak format of micro-periodicity for RVE-problems. Comput Methods Appl Mech Eng 2011;200:11–26. https://doi.org/10.1016/j.cma.2010.06.023.
[16] Harper LT, Qian C, Turner TA, Li S, Warrior NA. Representative volume elements for discontinuous carbon fibre composites – Part 1: Boundary conditions. Compos Sci Technol 2012;72:225–34. https://doi.org/10.1016/j.compscitech.2011.11.006.
[17] Yun J-H, Jeon Y-J, Kang M-S. Analysis of Elastic Properties of Polypropylene Composite Materials with Ultra-High Molecular Weight Polyethylene Spherical Reinforcement. Materials 2022;15:5602. https://doi.org/10.3390/ma15165602.
[18] Davari M, Rossi R, Dadvand P. Three embedded techniques for finite element heat flow problem with embedded discontinuities. Comput Mech 2017;59. https://doi.org/10.1007/s00466-017-1382-7.
[19] Liu H, Zeng D, Li Y, Jiang L. Development of RVE-embedded solid elements model for predicting effective elastic constants of discontinuous fiber reinforced composites. Mech Mater 2016;93:109–23. https://doi.org/10.1016/j.mechmat.2015.10.011.
[20] Temizer İ, Wriggers P. On the computation of the macroscopic tangent for multiscale volumetric homogenization problems. Comput Methods Appl Mech Eng 2008;198:495–510. https://doi.org/10.1016/j.cma.2008.08.018.
[21] Hill R. Elastic properties of reinforced solids: Some theoretical principles. J Mech Phys Solids 1963;11:357–72. https://doi.org/10.1016/0022-5096(63)90036-X.
[22] Geuzaine C, Remacle J-F. Gmsh: A 3-D finite element mesh generator with built-in pre- and post-processing facilities. Int J Numer Methods Eng 2009;79:1309–31. https://doi.org/10.1002/nme.2579.
[23] Lejeunes S, Bourgeois S. Une Toolbox Abaqus pour le calcul de propriétés effectives de milieux hétérogènes. 2011.
[24] Mote3D. Mote3D/Mote3D_toolbox 2023.